Chemistry & Biology
Article

The Novolactone Natural Product Disrupts the Allosteric Regulation of Hsp70

A. Quamrul Hassan,[2] Christina A. Kirby,[2] Wenlai Zhou,[2] Tim Schuhmann,[1] Roman Kityk,[3] D. Randal Kipp,[2] Jason Baird,[2] Jinyun Chen,[2] Yaoyu Chen,[2] Franklin Chung,[2] Dominic Hoepfner,[1] N. Rao Movva,[1] Raymond Pagliarini,[2] Frank Petersen,[1] Christopher Quinn,[2] Douglas Quinn,[2] Ralph Riedl,[1] Esther K. Schmitt,[1] Anne Schitter,[1] Travis Stams,[2] Christian Studer,[1] Pascal D. Fortin,[2] Matthias P. Mayer,[3] and Heather Sadlish[1,*]
[1]Novartis Institutes for BioMedical Research, Novartis Campus, 4056 Basel, Switzerland
[2]Novartis Institutes for BioMedical Research, 250 Massachusetts Avenue, Cambridge, MA 02139, USA
[3]Zentrum für Molekulare Biologie der Universität Heidelberg (ZMBH), DKFZ-ZMBH Alliance, Im Neuenheimer Feld 282, 69120 Heidelberg, Germany
*Correspondence: heather.sadlish@novartis.com
http://dx.doi.org/10.1016/j.chembiol.2014.11.007

SUMMARY

The highly conserved 70 kDa heat shock proteins (Hsp70) play an integral role in proteostasis such that dysregulation has been implicated in numerous diseases. Elucidating the precise role of Hsp70 family members in the cellular context, however, has been hampered by the redundancy and intricate regulation of the chaperone network, and relatively few selective and potent tools. We have characterized a natural product, novolactone, that targets cytosolic and ER-localized isoforms of Hsp70 through a highly conserved covalent interaction at the interface between the substrate-binding and ATPase domains. Biochemical and structural analyses indicate that novolactone disrupts interdomain communication by allosterically inducing a conformational change in the Hsp70 protein to block ATP-induced substrate release and inhibit refolding activities. Thus, novolactone is a valuable tool for exploring the requirements of Hsp70 chaperones in diverse cellular contexts.

INTRODUCTION

The highly conserved 70 kDa heat shock proteins (Hsp70) are fundamentally responsible for protein homeostasis through chaperoning normal folding, translocation, and trafficking events, as well as facilitating disaggregation and degradation processes. Some paralogs are constitutively expressed (heat shock cognates, e.g., HSPA8), while others are induced in the course of the stress response (e.g., HSPA1A/B). In eukaryotes, there are specialized isoforms found in each cellular compartment including the cytosol, endoplasmic reticulum, and mitochondria.

Behind Hsp70's protein-folding capabilities is a two-way allosteric control mechanism that links its nucleotide-binding domain (NBD) and substrate-binding domain (SBD) (Zuiderweg et al., 2013). Briefly, a transient interaction of the polypeptide substrate with Hsp70's SBD is controlled by the NBD nucleotide state; in the ATP-bound state the affinity is low, while ATP hydrolysis increases substrate affinity and reduces association and dissociation rates. The low basal rate of ATP hydrolysis, essential for Hsp70 chaperone activity, is stimulated by substrate binding and J-domain cochaperones (Hsp40s), which also aid substrate trapping. Nucleotide exchange is rate limiting for substrate release, such that nucleotide exchange factors (NEFs) control the lifetime of the Hsp70-substrate complex. Thus, these cochaperones are essential to maintain a continuous cycle of substrate binding, ATP hydrolysis, and substrate release (Mayer and Bukau, 2005). Despite a detailed understanding of this cycle in vitro, the precise relationships among the varied and redundant chaperone network components in a complex cellular environment are not fully understood.

In multiple diseases including cancer, as well as via neurodegeneration and aging, protein homeostasis becomes disrupted and inappropriate Hsp70 activity has been implicated as a key node for modulation. Both the high metabolic requirements of cancer cells, which stimulate the stress response, and Hsp70-mediated inhibition of cell death pathways are proposed to increase dependency on chaperones, stimulating efforts to inhibit Hsp70 function (Goloudina et al., 2012; Garrido et al., 2006; Beere et al., 2000). In polyglutamine disorders such as Huntington's disease, however, stimulating substrate binding to Hsp70 appears more beneficial than inhibition (Wang et al., 2013; Chafekar et al., 2012). Thus, the type of Hsp70 activity modulation required to alleviate a given disease is context dependent.

Understanding the precise role of Hsp70s in the cell is challenging due to the extensive redundancy of the chaperone network and the negative feedback mechanisms. The consequences of downregulating an individual isoform are limited; however, dual knockdown of both the cognate and inducible Hsp70s has been observed to phenocopy Hsp90 inhibition and cause extensive tumor-selective apoptosis (Powers et al., 2008; Schlecht et al., 2013). Pharmacological modulation of Hsp70s can occur within a timeframe that preceeds reequilibration of the chaperone network; this is a clear benefit, as demonstrated with geldanamycin, to elucidate the precise role of Hsp90 within the cell (Whitesell et al., 1994).

Identification of Hsp70 modulators began with the isolation of an inhibitory natural product (spergualin and its synthetic derivative, 15-deoxyspergualin) (Nadler et al., 1992). Despite high

hydrophilicity and a high affinity for ATP, two molecules targeting the ATP-binding pocket have been described, including an ATP-competitive inhibitor (VER-155008) (Williamson et al., 2009; Cho et al., 2011), while two compounds, gentamicin and geranylgeranylacetone, were reported to block substrate binding with low potency (Otaka et al., 2007; Yamamoto et al., 2010). In contrast, sites outside the ATP- and peptide-binding pockets have appeared more druggable. An analog of 15-deoxyspergualin, MAL3-101, and myricetin inhibit only J-domain-stimulated ATPase activity of Hsp70, suggesting binding outside the ATP-binding pocket (Chang et al., 2011; Fewell et al., 2004). MKT-077 also binds outside the nucleotide-binding pocket but only in the ADP-bound state (Rousaki et al., 2011), while an additional set of dihydropyrimidine derivatives, which stimulate or inhibit Hsp70, also have been described to bind adjacent to the J-domain binding site (Wisén and Gestwicki, 2008; Wisén et al., 2010). Binding sites in the SBD outside the peptide-binding pocket were proposed for pifithrin-μ (Leu et al., 2009); however, specific saturable binding was not observed in a biochemical study (Schlecht et al., 2013). A recent systematic approach to identify inhibitor-binding sites used a theoretical homology model of human Hsp70 (Rodina et al., 2013). This strategy was validated by the identification of allosteric inhibitors that bound to a pocket in the NBD (Kang et al., 2014; Taldone et al., 2014). Although a number of the binding sites have been revealed, a clear mechanistic understanding of the mode of inhibition has not been achieved for most of the above-mentioned compounds.

Here, we identify and characterize a fungal metabolite, novolactone, which uses a mechanism to disrupt the allosteric regulation of Hsp70 proteins. The covalent means of inhibition as well as its potency make novolactone a valuable tool to dissect and elucidate the role of cytoplasmic and ER Hsp70s in the cellular chaperone network.

RESULTS

Genome-wide Studies in Yeast Identify a Natural Product that Modulates Hsp70

The genetic tractability and evolutionary conservation of *S. cerevisiae* has enabled development of a powerful chemogenomic profiling approach to identify the pathways modulated by small molecules in a complex cellular environment (Smith et al., 2010; Hoepfner et al., 2014). Briefly, a pool of heterozygous or homozygous deletion strains entailing the ~6,000 genomic open reading frames is treated with the compound of interest. The sensitivity of each strain to the compound compared to the pool is plotted relative to the statistical sensitivity of that strain across thousands of chemically diverse scaffolds (*Z* score). In the simplest case of a classic enzymatic inhibitor, the single strain in the haploinsufficient pool (haploinsufficient profiling [HIP] assay) that represents the molecular target of that compound is more sensitive and, thus, shows a growth disadvantage. A second assay (homozygous profiling [HOP] assay) uses the homozygous deletions of the nonessential genes and, in a similar manner, can provide insight into the compensating pathways and/or synthetic lethal interactions with the compound target.

Novolactone was identified as a potential modulator of the chaperone network with an unprecedented profile among ~3,700 compounds evaluated (Figure 1A). In the HIP assay, heterozygous strains sensitive to the compound include ScHsp70, an Hsp70 NEF (SSE1), a ScHsp90 cochaperone (CNS1), and the stress-induced heat shock factor (HSF1) (Figure 1B). Several additional chaperone network components are sensitive in the HOP assay, including the Hsp90 cochaperones, STI1 and CPR7, and the protein disaggregase, HSP104. Cellular processes that rely heavily on the chaperone network are highlighted in both the HIP and HOP assays, including nuclear transport (NUP145, NUP85, and HEH2), the prefoldin complex (GIM5), and ER translocation (SEC66), further supporting the hypothesis that novolactone inhibits a key node. Importantly, the HIP HOP profile of novolactone is distinct from that of Hsp90 inhibitors, suggesting that Hsp90 is not the molecular target (Figures 1C and 1D).

In an independent approach, randomly mutagenized haploid yeast strains resistant to inhibitory concentrations of novolactone were characterized. Screening a genomic library prepared from one clone identified SSA1, one of four cytoplasmic members of the Hsp70 family. The remaining mutants yielded eight discrete amino acid alterations in SSA1, and representative strains for each demonstrated 2- to 8-fold resistance to novolactone compared to the unmutated parental strain (Figure 1E). Expression of representative SSA1 mutations in the parental yeast strain recapitulated the resistance, indicating a dominant mechanism (Figure 1F). Interestingly, all mutations caused single amino acid replacements in the SBD of the Hsp70 protein (Figure 1G). Taken together, these yeast-based unbiased genome-wide approaches clearly identify the Hsp70 protein family as a potential molecular target for novolactone.

Novolactone Irreversibly Inhibits HSP40-Stimulated Activities of Hsp70 In Vitro

To evaluate whether novolactone affects Hsp70 function, we assessed the impact on substrate refolding in vitro. Heat-denatured firefly luciferase was refolded in the presence of human Hsp70 (HSPA1A), the J-domain cochaperone HSP40 (DNAJB1), the NEF APG-2 (HSPH2/HSPA4), and novolactone over time. As shown in Figure 2A, there was a clear dose-dependent effect of novolactone on luciferase refolding with a maximal inhibition of ~90%.

To elucidate how novolactone inhibits HSPA1A chaperone activity, we next evaluated the effect on steady-state ATPase activity in the absence and presence of HSP40 (Figure 2B). Surprisingly, in the absence of HSP40, novolactone stimulated the steady-state ATPase activity of HSPA1A in a dose-dependent manner to a maximum level of 1.8-fold the activity in the absence of compound. In the presence of HSP40, however, novolactone inhibited the steady-state ATPase activity by ~70% (IC_{50} of 0.25 μM). A similar inhibition was observed with a 10:1 ratio of HSP40:HSPA1A, suggesting that novolactone inhibits HSP40-dependent ATPase activity, but is not competitive with HSP40. As inhibition could be mediated through competition with ATP, the effect of novolactone was assessed in the presence of increasing ATP concentrations. Inhibition of ATPase activity remained unchanged, indicating the compound does not compete with ATP (Figure 2C) and consistent with its stimulatory effect in the absence of HSP40. Interestingly, the ATPase activity was inhibited to a lesser degree (~70%) compared to the refolding activity (~90%).

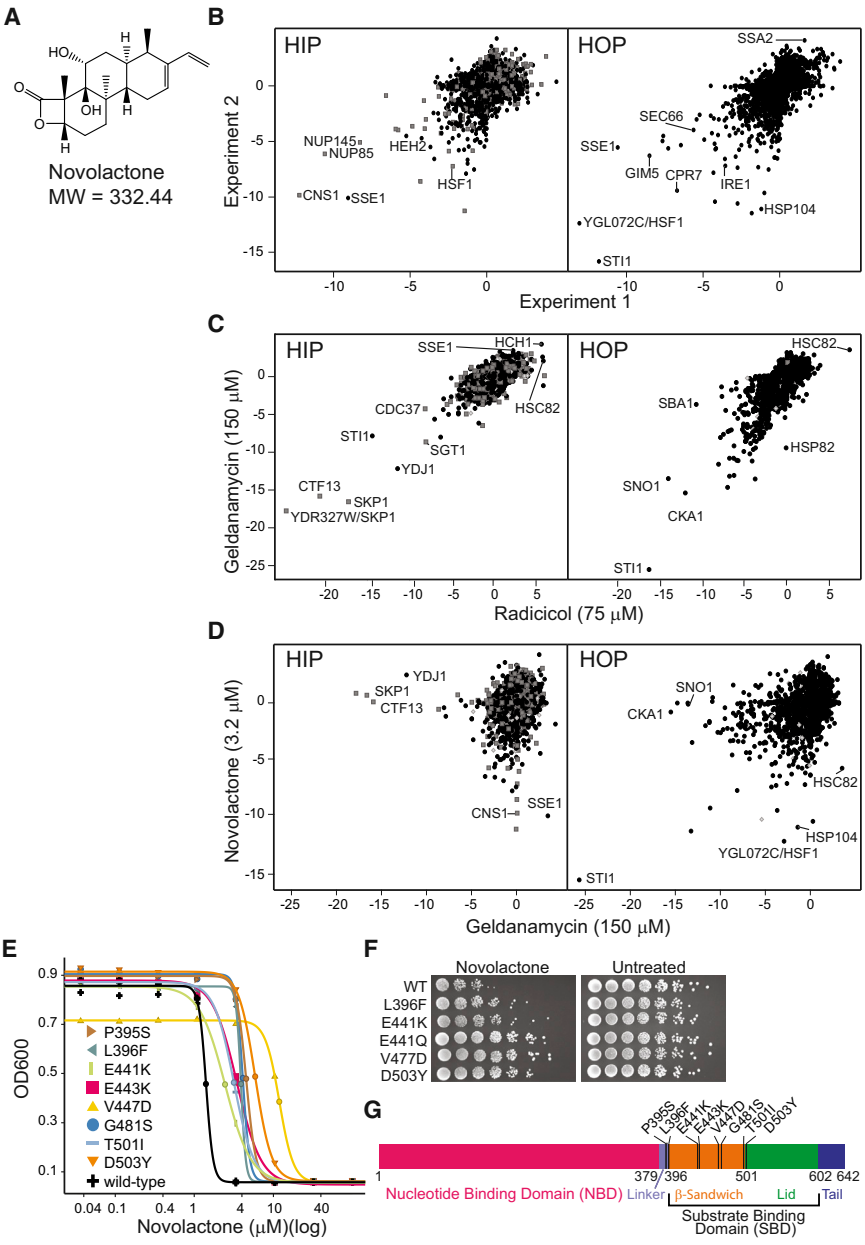

Figure 1. Genome-wide Yeast Assays Implicate Hsp70 Proteins as the Target of Novolactone

(A) Novolactone structure.

(B) Two independent HIP and HOP profiling experiments of novolactone are plotted using statistical significance of relative strain sensitivity (*Z* score, see Experimental Procedures). Strains essential for viability (gray boxes) and nonessential (black circles) are indicated. Commonly affected deletion strains involving chaperone networks are highlighted.

(C) Comparison of the HIP HOP *Z* scores for geldanamycin and radicicol indicate both Hsp90 inhibitors have similar chemogenomic profiles.

(D) The lack of alignment of the novolactone HIP HOP profile (*Z* score) with that of geldanamycin indicates the compounds have different molecular targets.

(E) Isolated genomic mutants are less sensitive to novolactone compared to the parental strain at the peak of logarithmic growth (16 hr). Individual strains were grown in rich media in a dose response of the compound. A representative data set from three technical replicates is shown.

(F) The mutations confer a dominant phenotype. Mutated SSA1 expressed from a plasmid transformed into wild-type cells led to resistance to novolactone (1.5 μM). Representative data set from at least two independent replicates is shown.

(G) Hsp70 domain architecture with SSA1 numbering. Resistant mutations (black lines) localized to the β sandwich domain.

The kinetics of novolactone inhibition of the ATPase activity was assessed after preincubating the compound with HSPA1A for 0, 30, or 60 min (Figure 2D). Remarkably, a 30 min preincubation led to a significant increase (5- to 10-fold) in novolactone potency, although the residual ATPase activity (~30%) remained unchanged with longer incubations. We assessed the reversibility of the time-dependent inhibition by preincubating HSPA1A (60 min) with a 10-fold molar excess of novolactone to allow full complex formation. Excess compound was removed by gel filtration and the compound-protein complex was diluted to promote dissociation, prior to evaluating the ATPase activity recovery. The time course of ADP production was linear and did not follow a model for reversible inhibition (recovery fit), indicating that ATPase activity did not increase over time as would be expected in a dissociation of the compound-protein complex (Figure 2E). These data suggest that the inhibition of HSPA1A's ATPase activity by novolactone is irreversible.

Novolactone Inhibits Hsp70 through a Covalent Interaction with Glu444

The dramatic effect of preincubation and the irreversibility of the novolactone inhibition suggest that the mechanism involves a covalent interaction. Indeed, through liquid chromatography-mass spectrometry (LC-MS) analysis of the HSPA1A protein in the presence or absence of novolactone, we could observe a difference in mass indicative of a covalent adduct (Figure S1A available online). Importantly, there was no mass difference for BSA in the presence of novolactone, suggesting a selective covalent interaction. To characterize the adduct, HSPA1A protein in the presence or absence of the compound was digested with proteases and the resulting pattern identified Glu444 as the single modification site (Figure S1B). Interestingly, mutation of the homologous yeast residue (*Sc*SSA1-E441K) was identified as enabling resistance (see above).

The most likely reactive moiety for covalent adduct formation in the novolactone structure is the lactone ring. Methanolic treatment opens the ring to form methylnovolactone, which was observed to be much less effective than novolactone in inhibiting

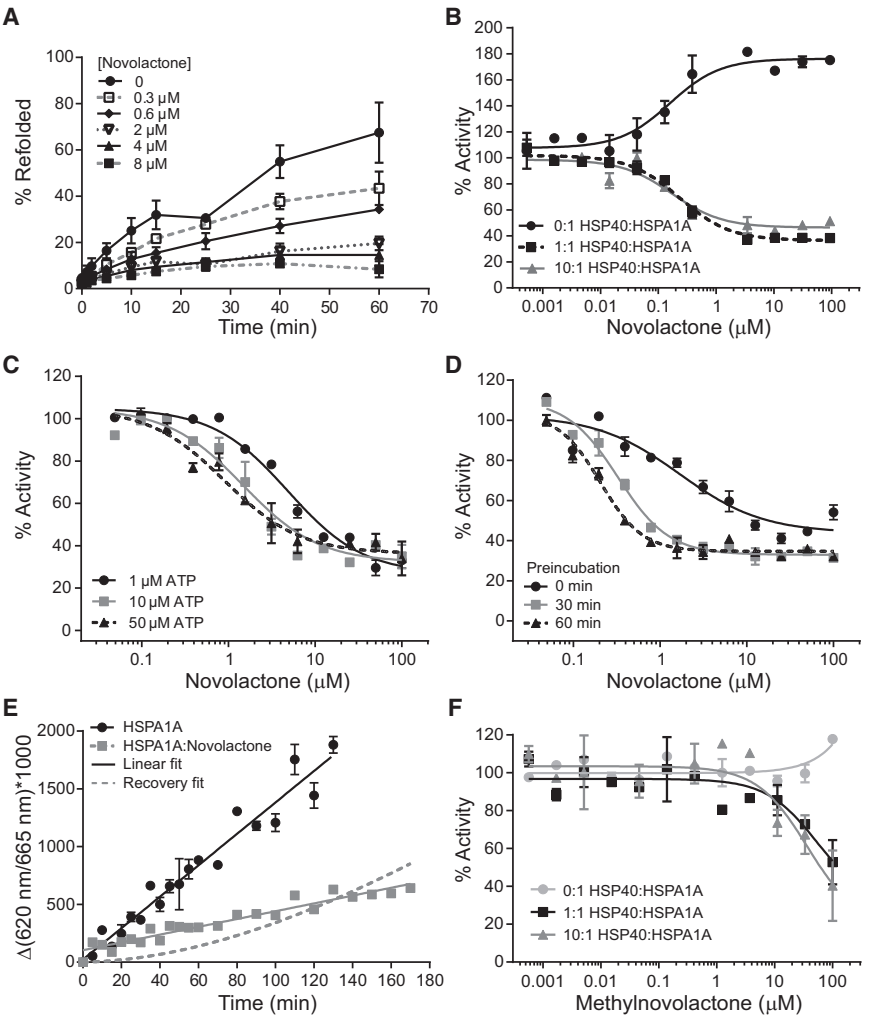

Figure 2. Novolactone Irreversibly Inhibits Luciferase Refolding and ATP Hydrolysis

(A) Luciferase-refolding activity of HSPA1A in the presence of 0 μM (●), 0.3 μM (□), 0.6 μM (◆), 2 μM (▽), 4 μM (▲), and 8 μM (■) novolactone.

(B) ATPase activity in response to novolactone in the absence (●) and presence of 1:1 (■) or 10:1 (▲) HSP40.

(C) Novolactone inhibition of ATPase activity in the presence of 1 μM (●), 10 μM (■), and 50 μM (▲) ATP.

(D) ATPase activity after preincubation with novolactone for 0 min (●), 30 min (■), and 60 min (▲).

(E) ATPase activity as a ratio of 620/665 nm of HSPA1A alone (●) and HSPA1A-novolactone complex (■) after 60 min preincubation of HSPA1A with novolactone (10-fold excess) followed by removal of unbound compound and 100-fold dilution in buffer. Solid lines represent linear fits and the dotted line represents the predicted fit for recovery of activity resulting from novolactone dissociation.

(F) ATPase activity in response to methylnovolactone in the absence (●) and presence of 1:1 (■) or 10:1 (▲) HSP40. Data are means from three independent experiments; error bars show the SE.

HSPA1A ATPase activity (Figures 2F and S2A). Further, HIP HOP analysis demonstrated little cellular activity compared to novolactone, confirming the critical role of the lactone ring in mediating the covalent adduct (Figure S2B).

Biochemical Dissection of the Molecular Mechanism of Novolactone

To clarify the molecular mechanism by which novolactone inhibits the HSPA1A chaperone activity, we followed the surprising observation that novolactone stimulated the basal ATPase rate but partially inhibited the HSP40-stimulated ATPase rate (Figure 2B). There are three possibilities for such an effect: (1) novolactone could directly disrupt the interaction of the J-domain of HSP40 with the NBD of HSPA1A; (2) in the presence of a J-domain cochaperone, nucleotide exchange becomes rate limiting for the steady-state ATPase activity of Hsp70s (Brehmer et al., 2001; Gassler et al., 2001) and inhibition of nucleotide exchange would limit the observable HSP40-stimulated ATPase rate; or (3) novolactone could interfere with the allosteric mechanism of HSPA1A. The first hypothesis is unlikely, however, because complete inhibition of the ATPase activity could not be achieved even at very high novolactone concentrations, and there was no competition effect with HSP40 (see above).

To test the second hypothesis we measured the influence of novolactone on nucleotide exchange by determining the ADP dissociation rate in the absence and presence of the APG2 NEF (Dragovic et al., 2006; Raviol et al., 2006), using the fluorescent ADP analog N8-(4N′-methylanthraniloylaminobutyl)-8 amino-adenosine 5′-diphosphate (MABA-ADP) (Theyssen et al., 1996). The measured exchange rates were nearly identical (Figure 3A), demonstrating that novolactone has no effect on ADP release. Alternatively, novolactone may directly affect γ-phosphate cleavage; thus, we determined HSPA1A's ATPase rate under single-turnover conditions. Complexes of HSPA1A with ATP were isolated, and in the absence of compound we measured a basal ATP hydrolysis rate of 3.3×10^{-4} s^{-1}, consistent with previous observations (Gassler et al., 2001). In the presence of novolactone, we observed a concentration-dependent stimulation of this single-turnover ATPase rate by 10% to 40% (Figures 3B and S3), consistent with the steady-state ATPase assays. The basal single-turnover ATPase rate was stimulated 78-fold (2.6×10^{-2} s^{-1}) by HSP40, and was only slightly inhibited upon the addition of novolactone. In the steady-state ATPase assays, novolactone was more potent after preincubation with HSPA1A; however, this is not possible with the HSPA1A •ATP complexes. Thus, we first incubated HSPA1A with a 4-fold molar excess of novolactone to form the covalent adduct and subsequently isolated HSPA1A •ATP complexes. Even under these conditions, the HSP40-stimulated ATPase activity was only reduced to 57% of the activity of the untreated HSPA1A sample, contrasting with the ~70% inhibition seen in the steady-state assay.

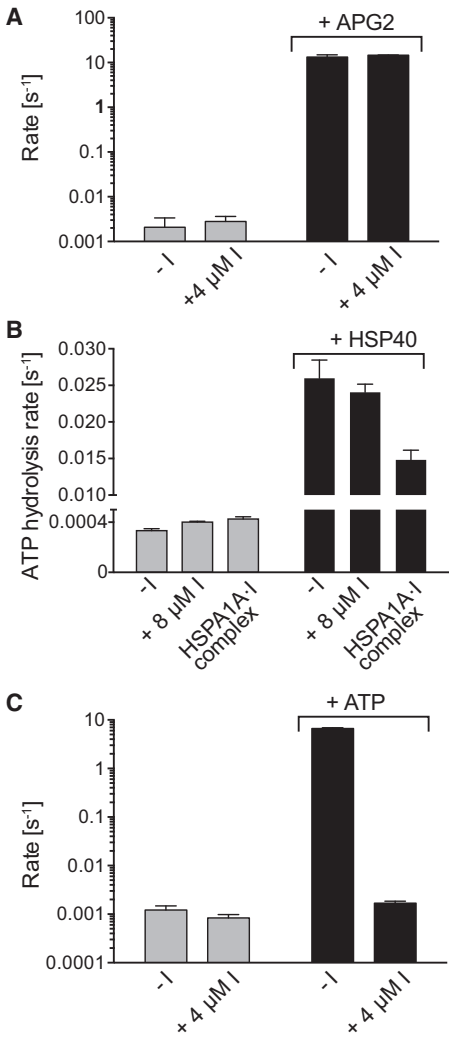

Figure 3. Novolactone Inhibits the Allosteric Control Mechanism of HSPA1A

(A) Novolactone influences neither basal (gray bars) nor APG2-stimulated (black bars) nucleotide exchange rates. Nucleotide exchange was measured in the absence and presence of novolactone (−I, +4 μM I) by following the change in fluorescence of the fluorescent ADP analog MABA-ADP (Theyssen et al., 1996). Traces were fitted by single-exponential decay functions.

(B) Novolactone partially inhibits HSP40-stimulated rate of γ-phosphate cleavage. ATPase activity was measured under single-turnover conditions in the absence (gray bars) or presence of HSP40 (black bars), absence or presence of novolactone (−I, +8 μM I), and with HSPA1A •ATP complexes that were isolated from novolactone-pretreated HSPA1A (HSPA1A •I complex).

(C) Novolactone prevents the stimulation of substrate release by ATP. Substrate dissociation was measured in the absence (gray bars) and presence of ATP (black bars) and absence and presence of novolactone (−I, +4 μM I) by following the decrease of fluorescence of a fluorescent-labeled peptide (dansyl-NRLLLTG). Traces were fitted by single-exponential decay functions. Error bars represent the SE of two to four experiments.

It was shown previously that full stimulation of the ATPase activity of Hsp70s requires the synergistic action of a J-domain protein and a substrate (Karzai and McMacken, 1996; Barouch et al., 1997), but that some J-domain proteins can deliver both signals in the absence of a substrate by interacting simultaneously with the NBD and the SBD (Laufen et al., 1999). Furthermore, full stimulation of the ATPase activity requires an intact interdomain communication between the NBD and SBD. We hypothesized that the effect of novolactone on the HSP40-stimulated ATPase activity could be explained by an interference with this interdomain communication, and evaluated the effect on ATP-stimulated peptide release (Figure 3C). In the absence of ATP, peptides dissociate from HSPA1A at a rate of 1.2×10^{-3} s^{-1}, and novolactone had little effect on this parameter. ATP stimulates this rate by more than three orders of magnitude to 6.6 s^{-1}; however, in the presence of novolactone, the ATP-stimulated rate of peptide dissociation was drastically reduced to 1.5×10^{-3} s^{-1}. Therefore, novolactone increased the half-life of the HSPA1A-peptide complex 4,500-fold from 0.11 to 471 s. Together these data strongly suggest that novolactone impairs the allosteric control mechanism between the SBD and the NBD of HSPA1A.

Structural Analysis of the Hsp70 SBD with Novolactone

To validate this hypothesis and gain insight into the novolactone-binding pocket, we used X-ray crystallography to determine the structures of the apo (Protein Data Bank [PDB] ID 4WV5) and covalently modified (PDB ID 4WV7) HSPA1A SBD (395–543) to 2.0 and 2.4 Å resolution, respectively. The structures contained the SBDβ subdomain as well as αA and αB of the SBDα subdomain (Figure 4A; Table S1). The overall fold of the HSPA1A SBD structure compared well with that of the previously described DnaK SBD structure (Zhu et al., 1996), a protein sharing strong homology with HSPA1A, with an rmsd of 0.503 Å when comparing the SBDβ subdomains (residues 395–504). Changes between novolactone-bound HSPA1A and DnaK SBDs also reflected those seen between novolactone-bound and apo HSPA1A SBDs. In both HSPA1A SBD structures the C-terminal portion of helix αB, including residues Lys539-Glu543, could be seen binding in the substrate-binding pocket, as has been observed previously for similar structures (Jiang et al., 2005; Morshauser et al., 1999; Wang et al., 1998).

Comparison of the apo HSPA1A SBD structure to that of the novolactone-bound revealed a covalent linkage at Glu444 within $\mathcal{L}_{4,5}$ (Figures 4B and 4C). The binding pocket for this modification was defined by multiple van der Waals interactions with residues Ala397-Leu399 of β1, Leu456 of β5, Gly484-Ile485 of $\mathcal{L}_{6,7}$, Ile480 of β6, Ile503-Asp506 of $\mathcal{L}_{\alpha,\beta}$, and Leu510 of αA. Water-mediated hydrogen bonds between the hydroxyl group of the novolactone and the backbone amide and carbonyl of Leu399 also were present in the B molecule of the structure. Further effects of this modification included a repositioning of β7 and $\mathcal{L}_{6,7}$.

Residues within regions $\mathcal{L}_{4,5}$, $\mathcal{L}_{6,7}$, and β7 of the SBD have been shown previously to interact at the interface with the NBD in the ATP-bound open conformation of DnaK (Kityk et al., 2012; Figure 4D), a region implicated in the allosteric regulation of Hsp70s. The covalent modification of Glu444 would clearly disrupt this interface (Figures 4E and 4F), including the loss of a hydrogen bond between its side chain and the backbone amide of Asp152 within the IA subunit of the NBD. An additional hydrogen bond between the backbone amide of Leu486 within $\mathcal{L}_{6,7}$ to the side chain of Asp152 would be lost due to

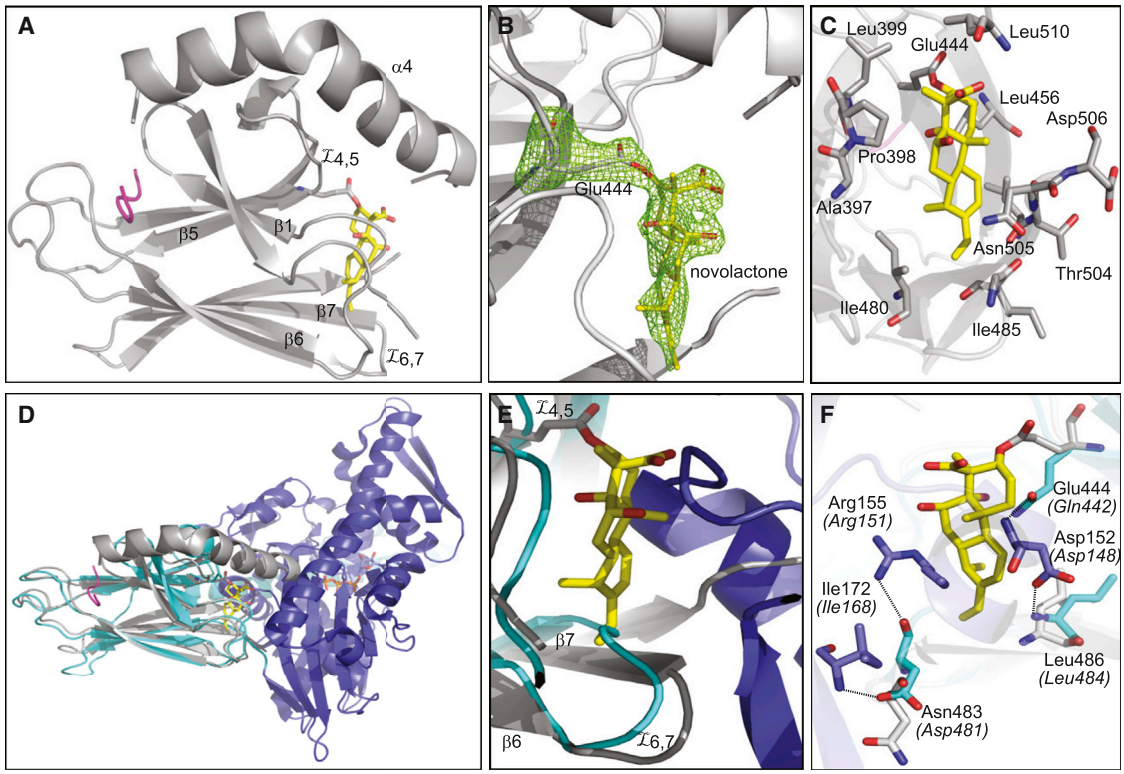

Figure 4. Crystal Structure of HSPA1A with Novolactone

(A) Crystal structure of HSPA1A SBD (gray) covalently modified by novolactone (yellow). The substrate-binding site is occupied by the C terminus of the protein (magenta).

(B) The unbiased electron density (Fo-Fc omit map contoured at 3σ) for novolactone bound to Glu444.

(C) Novolactone-binding site showing covalent modification of Glu444 as well as multiple residues involved in van der Waals interactions.

(D) Overlay of the crystal structures of the HSPA1A SBD (gray) and DnaK in the ATP-bound open conformation (PDB ID 4B9Q) (Kityk et al., 2012), containing both the NBD (blue) and SBD (cyan).

(E) Binding pocket from overlay showing steric clash between novolactone (yellow) and the NBD (blue) as well as the relocation of β7 and $\mathcal{L}_{6,7}$ in HSPA1A SBD (gray) compared to the DnaK SBD (cyan).

(F) Binding pocket from overlay showing key interactions between the NBD (blue) and SBD (cyan) of DnaK that would be disrupted upon novolactone binding. Residue numbering is for HSPA1A with the equivalent DnaK residue in parentheses.

the repositioning of this loop away from the NBD as well as steric interference of novolactone. Additionally, hydrogen bonding interactions between Asn483 within $\mathcal{L}_{6,7}$ to the backbone amide of Ile172 and from its backbone amide to the Arg155 side chain in the NBD would be disrupted. The equivalent residue in DnaK (Arg151) has been defined as a relay in determining the conformation of the SBD (Vogel et al., 2006a). Notably, the residues surrounding the compound-binding pocket in the crystal structure are homologs to those identified in the yeast mutagenesis approach (see above).

Recently, a crystal structure of the DnaK SBD in complex with a noncovalently interacting molecule, PET-16, was reported (Leu et al., 2014). Although much of PET-16 is solvent exposed, an acetylene linker directs a phenyl group into a portion of the binding pocket occupied by novolactone, supporting the potential for druggability. Importantly, aside from the results presented here, a comprehensive demonstration that a small molecule bound in this pocket disturbs the allosteric communication between NBD and SBD has not been reported previously.

Novolactone Is Selective for Cytosolic and ER-Localized Isoforms of Hsp70

We noted that the key interacting residues of novolactone, as identified by yeast mutagenesis and visualized by cocrystallization with the SBD, are conserved across both human and yeast species. Interestingly, the Glu444-binding site is a glutamine in all ribosome-associated and mitochondrial isoforms of Hsp70 (Figure S4). When this subtle substitution was introduced in the yeast SSA1 (E441Q), sensitivity to novolocatone was dramatically decreased (Figure 1F), indicating the compound is likely active against all cytosolic and ER-localized Hsp70 family members, but not ribosome-associated or mitochondrial isoforms.

To evalute this hypothesis, we took advantage of the yeast genetic malleability to generate a strain missing the redundant cytoplasmic Hsp70 isoforms (*Δssa2-4*). In this background compared to one with an intact chaperone network, there was an additional decrease in sensitivity for the SSA1-E441Q mutant (Figure 5). When the novolactone target residue in the ER-localized Kar2 was additionally mutated to a glutamine (E487Q), there was nearly a 100-fold shift in sensitivity compared to a wild-type

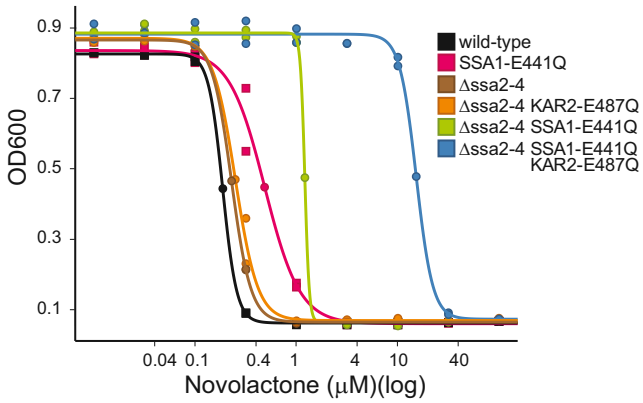

Figure 5. Sensitivity to Novolactone Requires Intact Cytosolic or ER-Localized Hsp70s

Yeast strains missing redundant cytosolic Hsp70s (Δ*ssa2-4*) and/or expressing Hsp70s missing the novolactone-reactive glutamine (cytosolic, SSA1-E441Q; ER-localized, KAR2-E487Q) were grown in rich media with compound dilutions. A representative data set with biological duplicates from two technical replicates is shown.

control. The residual activity of novolactone in this cellular context was similar to that of methylnovolactone on HSPA1A in vitro (Figure S2B), and may be attributed to a noncovalent interaction with the protein. Taken together, these data demonstrate that novolactone is selectively reactive against cytosolic and ER-localized Hsp70 family members.

Novolactone Disrupts Hsp70 Protein Function in Mammalian Cells

The chemogenomic profiling indicates novolactone affects the chaperone network in yeast, and, while the compound inhibits the human HSPA1A in vitro, we wanted to evaluate whether it has a selective effect on Hsp70s in mammalian cells. Novolactone was tested in human cells alongside an ATP-competitive inhibitor of Hsp70s, VER-155008, and the Hsp90 inhibitor, HSP990, for comparison (Figure 6A; Williamson et al., 2009; Menezes et al., 2012). In cells, Hsp70s and Hsp90s cooperate in the folding of several key regulatory proteins; thus, their activities are highly connected. We selected two lung cancer cell lines that express the known HSP90 client proteins EGFR and MET: (1) EBC-1 (EGFR wild-type, MET amplified), and (2) HCC827 (EGFR oncogenic E746-A750 deletion, MET wild-type). Treatment of either cell line with HSP990 led to increased degradation of EGFR and MET proteins, as well as stimulation of HSPA1A and c-PARP, a marker of apoptosis, consistent with previous reports (Figure 6A; Menezes et al., 2012). In comparison, VER-155008 had little effect on these Hsp90 client proteins, but at higher concentrations stimulated c-PARP and HSPA1A. Novolactone treatment led to reduced levels of Hsp90 client proteins and induction of both HSPA1A and c-PARP. This pattern of events resembled that seen with the Hsp90 inhibitor, but also was consistent with inhibition of both HSPA1A and HSPA8 (Powers et al., 2008). No covalent adduct was observed upon incubation of novolactone with purified HSP90AB1 (Figure S5), and the effect was consistent with inhibition of all cytosolic forms of the Hsp70s, as predicted by the reactivity of novolactone. Further, the induction of HSPA1A would simply reflect the novolactone-mediated inhibition of HSPA8.

To confirm the reactivity of novolactone with both isoforms of mammalian Hsp70, we utilized an HCT116 cell line generated to inducibly knock out HSPA8. As expected, HSPA1A was clearly upregulated in response to HSPA8 inactivation (Figure 6B; compare WT to HSPA8$^{-/fl}$). In the presence of novolactone, the depletion of Hsp90 client proteins (HER2 and CDK4) was significantly enhanced when combined with the HSPA8 knockout (Figure 6C). Thus, the response profile of novolactone in mammalian cells is consistent with a selective inhibition of both the inducible and constitutive Hsp70 proteins in the chaperone network.

DISCUSSION

Using a combination of cellular and in vitro approaches, we have identified and characterized the natural product, novolactone, as having an unprecedented ability to affect the cellular chaperone network through allosterically blocking interdomain communication and, consequently, ATP-induced substrate release by cytostolic and ER-localized Hsp70 proteins.

To understand the functional consequences of the covalent adduct, it is important to appreciate that Hsp70s undergo dramatic conformational changes when progressing through the ATPase cycle (Figure 7A). In the nucleotide-free state, the NBD and SBD are connected only by a flexible linker. Upon ATP binding by the NBD, the SBD dissociates into the β sandwich subdomain and the α-helical lid subdomain and docks onto two faces of the NBD. Glu444 is exactly at the interface between the β sandwich subdomain and the NBD, and the novolactone adduct induces a conformational change that appears incompatible with the interaction of the two domains (Figure 4E). The contacts between the β sandwich subdomain and the NBD are essential to induce the opening of the substrate-binding cleft and substrate release (Figure 7A), as has been shown in several studies (Jiang et al., 2005; Liu and Hendrickson, 2007; Montgomery et al., 1999; Smock et al., 2010; Vogel et al., 2006a).

The disruption of interdomain communication also explains two observations that initially seemed odd. First, novolactone increased the basal ATPase rate in steady-state and single-turnover experiments (Figures 2B, 3B, and S3). All known single amino acid replacement variants of Hsp70s, at the interface between the β sandwich subdomain of the SBD and the NBD and that block interdomain communication, also have an increased basal rate of ATP hydrolysis (Montgomery et al., 1999; Smock et al., 2010; Vogel et al., 2006a, 2006b). These observations suggest that a functional interdomain communication is required for the low basal ATPase activity of Hsp70s. This is also consistent with a recent nuclear magnetic resonance (NMR) study, which suggested that the hydrolysis competent conformation of Hsp70s is only reached by a tug-of-war between the β sandwich subdomain and NBD (Zhuravleva et al., 2012).

The second puzzling observation was that novolactone inhibited the HSP40-stimulated ATPase rate in steady-state ATPase assays by 70%, while the inhibition in single-turnover assays was less than 50% even when nearly 100% of HSPA1A was modified, as verified by mass spectrometry (MS) (Figure S1). In steady-state assays, a new ATP must bind after hydrolysis to

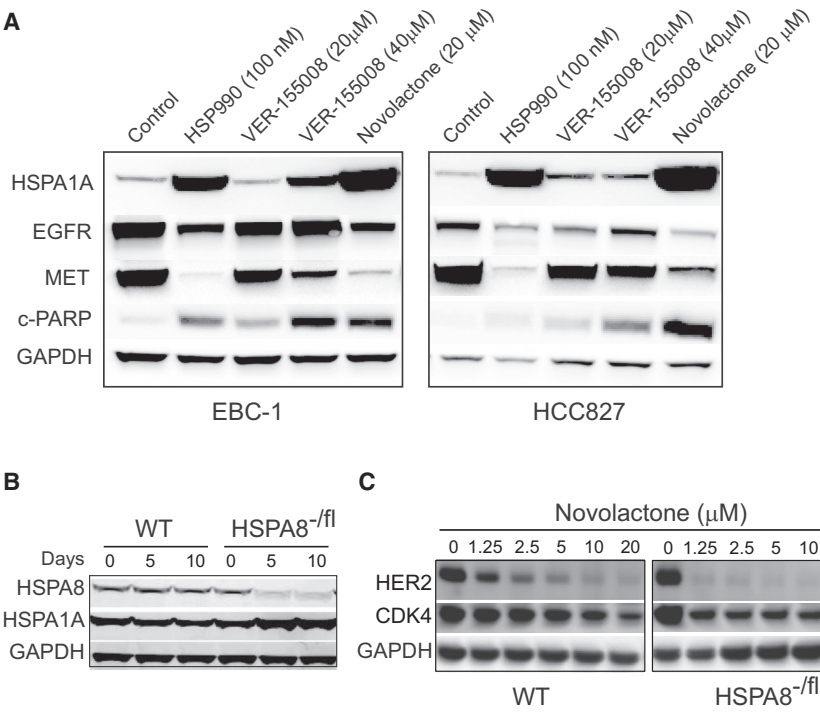

Figure 6. Novolactone Treatment of Cancer Cells Leads to Hsp90-Inhibitor-like Downstream Effects

(A) EBC-1 (EGFR wild-type, MET amplified) and HCC827 (EGFR oncogenic E746-A750 deletion, MET wild-type) cells were treated with an Hsp90 inhibitor (HSP990), an ATP competitive inhibitor of Hsp70s (VER-155008), or with novolactone. Western analysis of EGFR, c-PARP, HSP70, and GAPDH after 24 hr treatment.

(B) Western analysis of HSPA8 and HSPA1A at different time points after HSPA8$^{-/fl}$ HCT116 cells were transduced with CRE adenovirus.

(C) Western analysis of ERBB2 and CDK4 3 days after HSPA8$^{-/fl}$ HCT116 cells were transduced with CRE adenovirus, then followed by 24 hr of treatment with serial dilutions of novolactone.

enable the next round of hydrolysis. The ATP binding occurs via a two-step mechanism that, for reasons not yet understood, requires substrate release before a hydrolysis-competent conformation can be assumed. Under these conditions, HSP40 is able to provide both signals necessary for triggering ATP hydrolysis in HSP70; the J-domain interacts with the NBD, and a region C-terminal to the J-domain acts as the substrate. As we have shown here, however, novolactone blocked the ATP-stimulated substrate release. Therefore, HSP40 dissociation (i.e., substrate release) prior to rebinding to trigger the second round of ATP hydrolysis was likely the rate-limiting step in steady-state ATPase assays. In single-turnover assays, HSP40 dissociation and rebinding was not necessary, explaining the reduced impact of novolactone.

The initial binding of novolactone for the Hsp70-binding pocket seems to be driven by a series of noncovalent interactions, which enables proper positioning of the compound. The lactone is the key reactive moiety of novolactone, and it likely undergoes an irreversible transesterification reaction with the carboxylic acid of Glu444 (Figure 7B). The resulting stable ester bond would subsequently induce or stablize a change in conformation, forcing the Hsp70 protein to adopt a nonfunctional state. One can envisage two scenarios to explain the long preincubation time required for maximal inhibitory activity: (1) it may take time for the compound to be properly positioned to enable the covalent reaction, or (2) the covalent interaction induces a conformational change that takes time to have functional effects.

ScHsp70 (SSA1) was identified as the primary target of novolactone in a cellular context using unbiased genome-wide mutagenesis, while cocrystallization of HSPA1A and novolactone yielded unequivocal identification of Glu444 as the site of covalent modification. Sequence comparisons suggested that cytoplasmic and ER-localized isoforms were targets of novolactone. This was confirmed in yeast where, upon accounting for the redundancy of the cytosolic Hsp70s, substitution of the reactive glutamate in the remaining proteins was sufficient to dramatically shift the sensitivity to novolactone. In mammalian cells, novolactone stimulated depletion of Hsp90 client proteins and induced apoptosis, a selective and relevant response demonstrating the applicability of the compound to mammalian systems.

Selective pharmacological inhibitors can be extremely useful in dissecting the precise role of individual chaperones within the cellular chaperone network. While several compounds have been reported to bind and inhibit Hsp70s, novolactone is one of the few where the mechanism of action has been comprehensively delineated at both the molecular level and in a cellular environment. Novolactone is, thus, a valuable tool for evaluating Hsp70 as a potential drug target in different cellular contexts (Frye, 2010).

SIGNIFICANCE

The Hsp70 protein family plays an integral role in proteostasis and, as such, has been implicated as a key node in numerous diseases. There remains some uncertainty as to how the pathway should be modulated, however, as benefit has been reported with both stimulation and/or inhibition of Hsp70 in various disease contexts. One of the greatest challenges to deconvoluting the role in the cellular chaperone network is the extensive reduncancy and intricate regulation of Hsp70s, which inherently limit the application of genetic tools. We have characterized a natural product, novolactone, which can assist in determining the requirements of cytosolic and ER-localized Hsp70s under different conditions. Novolactone covalently binds a discrete residue (Glu444) at the interface of the SBD and the NBD to inhibit substrate-folding activities through a novel allosteric mechanism. The observed increase in ATP hydrolysis upon novolactone treatments also validates current models of Hsp70 interdomain regulation with critical interactions between the β sandwich subdomain and NBD. Further, the

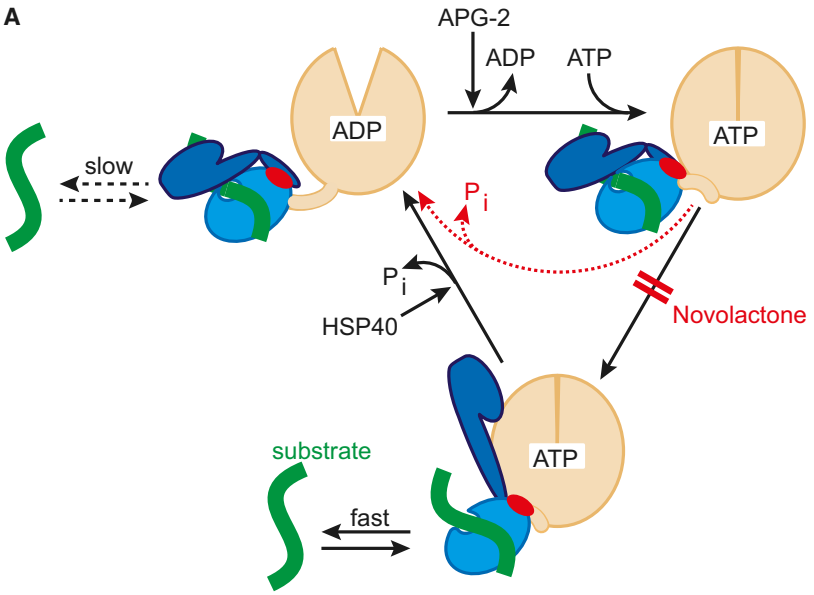

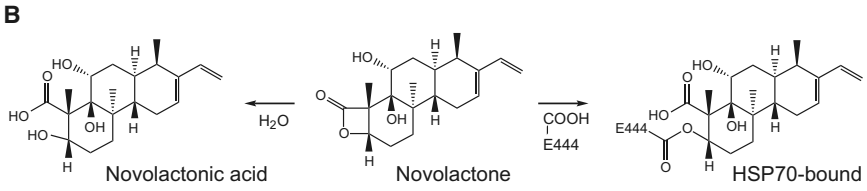

Figure 7. Mode of Action of the Hsp70 Inhibitor, Novolactone

(A) Hsp70s undergo several distinct conformational changes while progressing through the ATPase cycle. In the ADP-bound state substrate association and dissociation rates are low. After AGP-2-stimulated ADP dissociation, ATP binding to the NBD leads to docking of the β sandwich subdomain of the SBD to the NBD with subsequent opening of the substrate-binding pocket. Novolactone binding interferes with the interaction of the β sandwich domain with the NBD and, thus, disturbs the allosteric opening of the substrate-binding cleft. The HSP40-mediated stimulation of the ATPase activity is also strongly reduced (red dotted arrow).

(B) Proposed reactivity of novolactone. Under physiological conditions, the lactone degrades to the free acid (left), which, like methylnovolactone, would be essentially inactive. In the proximity of Glu444, however, transesterification is favored resulting in covalent bond formation with the protein (right).

conservation of the novolactone-binding pocket from humans to yeast cytosolic and ER-localized Hsp70 isoforms provides versatility for potential applications.

EXPERIMENTAL PROCEDURES

HIP HOP Assay

The HIP HOP assay and microarray analysis were performed as described previously (Pierce et al., 2007).

Yeast Strains

A BY4743 strain containing deletions of multiple drug resistance genes (Δ8 - *snq2::KanMX; pdr5::KanMX; pdr1::NAT1; pdr3::KanMX; yap1::NAT1; pdr2Δ; yrm1Δ; yor1Δ*) was used for all experiments and modified further as needed using standard techniques.

ATPase Assay

ATP (1 μM) and HSP40 were mixed together and reaction was initiated with addition of HSPA1A at the desired concentration in reaction conditions of 50 mM HEPES, pH 7.3, 10 mM $MgCl_2$, 20 mM KCl, 2 mM TCEP, and 0.01% BSA. The reaction was stopped with ADP-Glo™, and ADP detection reagent (Promega) was added prior to reading luminescence with the EnVision plate reader (Perkin Elmer). For determining dissociation kinetics, a 10-fold excess of novolactone was incubated with HSPA1A for 60 min prior to removal of unbound compound and 100-fold dilution of the HSPA1A-novolactone complex in reaction buffer. Equal proportions of the complex (40 nM) was mixed with ATP (20 μM), 400 nM HSP40, and 1% DMSO in reaction buffer, and the ATPase activity was monitored using the HTRF Transcreener ADP detection kit (Cisbio).

Single-Turnover ATPase Assay

HSPA1A ATPase activity under single-turnover conditions in the absence and presence of HSP40 (2 μM) was determined as described previously (Mayer et al., 1999).

Substrate Dissociation Kinetics

Substrate dissociation kinetic measurements, in the presence and absence of ATP, were performed as described previously (Gassler et al., 2001).

Nucleotide Exchange Kinetics

Nucleotide exchange kinetic measurements were performed as described previously (Gassler et al., 2001), except that APG2 was used as an NEF. When appropriate, HSPA1A was preincubated with novolactone.

Luciferase-Refolding Assay

Firefly luciferase was mixed with HSPA1A, HSP40, and APG2 and thermally denatured at 42°C. At given time points after shifting the reaction to 30°C, aliquots were mixed with luciferin and luminescence was measured in a Biolumat (Berthold). Where appropriate, novolactone was added to the reaction prior to unfolding.

Covalent Modification and MS

For intact MS, novolactone (10-fold excess) was incubated with a mixture of HSPA1A and BSA at room temperature for 60 min. Before and after compound treatment, an aliquot was analyzed on a Waters Micromass ZQ mass spectrometer. For tandem mass spectrometry (MS/MS) analysis, samples were treated with LysC (Roche), both LysC and AspN (Roche), or trypsin enzyme at room temperature overnight. Concentrated protein digests were then analyzed by LC-MS with an Agilent 1200 capillary LC stack using an Acquity BEH C-18 1.0 × 100 mm chromatography column and a Thermo Scientific LTQ mass spectrometer. Mascot software was used for data analysis.

Compounds

Novolactone has been isolated as a secondary metabolite of a fungal strain closely related to *Aporospora terricola*. Methylnovolactone was generated by dissolving novolactone in methanol for 5 days and subsequently purified by reverse-phase chromatography. Structure elucidation was achieved by means of ESI-MS as well as 1D and 2D NMR spectroscopy.

Additional details are included in the Supplemental Experimental Procedures.

SUPPLEMENTAL INFORMATION

Supplemental Information includes Supplemental Experimental Procedures, five figures, and one table and can be found with this article online at http://dx.doi.org/10.1016/j.chembiol.2014.11.007.

ACKNOWLEDGMENTS

The authors acknowledge T. Aust for running the HIP HOP platform; M. Li for supplying HSPA1A protein; H. Zhai and D. Wall for MS image processing; M. Ponelle, A. Luneau, and L. Oberer for NMR structural analyses; R. Aichholz for novolactone stability testing; and N. Hentze for MS analysis. Use of the IMCA-CAT beamline 17-ID at the Advanced Photon Source was supported by the companies of the Industrial Macromolecular Crystallography Association through a contract with Hauptman-Woodward Medical Research Institute. Use of the Advanced Photon Source was supported by the U.S. Department of Energy, Office of Science, Office of Basic Energy Sciences, under Contract DE-AC02-06CH11357. This work was supported by the Deutsche Forschungsgemeinschaft (MA1278/4-1 to M.P.M.).

Received: January 16, 2014
Revised: October 11, 2014
Accepted: November 3, 2014
Published: December 24, 2014

REFERENCES

Barouch, W., Prasad, K., Greene, L., and Eisenberg, E. (1997). Auxilin-induced interaction of the molecular chaperone Hsc70 with clathrin baskets. Biochemistry *36*, 4303–4308.

Beere, H.M., Wolf, B.B., Cain, K., Mosser, D.D., Mahboubi, A., Kuwana, T., Tailor, P., Morimoto, R.I., Cohen, G.M., and Green, D.R. (2000). Heat-shock protein 70 inhibits apoptosis by preventing recruitment of procaspase-9 to the Apaf-1 apoptosome. Nat. Cell Biol. *2*, 469–475.

Brehmer, D., Rüdiger, S., Gässler, C.S., Klostermeier, D., Packschies, L., Reinstein, J., Mayer, M.P., and Bukau, B. (2001). Tuning of chaperone activity of Hsp70 proteins by modulation of nucleotide exchange. Nat. Struct. Biol. *8*, 427–432.

Chafekar, S.M., Wisén, S., Thompson, A.D., Echeverria, A., Walter, G.M., Evans, C.G., Makley, L.N., Gestwicki, J.E., and Duennwald, M.L. (2012). Pharmacological tuning of heat shock protein 70 modulates polyglutamine toxicity and aggregation. ACS Chem. Biol. *7*, 1556–1564.

Chang, L., Miyata, Y., Ung, P.M., Bertelsen, E.B., McQuade, T.J., Carlson, H.A., Zuiderweg, E.R., and Gestwicki, J.E. (2011). Chemical screens against a reconstituted multiprotein complex: myricetin blocks DnaJ regulation of DnaK through an allosteric mechanism. Chem. Biol. *18*, 210–221.

Cho, H.J., Gee, H.Y., Baek, K.H., Ko, S.K., Park, J.M., Lee, H., Kim, N.D., Lee, M.G., and Shin, I. (2011). A small molecule that binds to an ATPase domain of Hsc70 promotes membrane trafficking of mutant cystic fibrosis transmembrane conductance regulator. J. Am. Chem. Soc. *133*, 20267–20276.

Dragovic, Z., Broadley, S.A., Shomura, Y., Bracher, A., and Hartl, F.U. (2006). Molecular chaperones of the Hsp110 family act as nucleotide exchange factors of Hsp70s. EMBO J. *25*, 2519–2528.

Fewell, S.W., Smith, C.M., Lyon, M.A., Dumitrescu, T.P., Wipf, P., Day, B.W., and Brodsky, J.L. (2004). Small molecule modulators of endogenous and co-chaperone-stimulated Hsp70 ATPase activity. J. Biol. Chem. *279*, 51131–51140.

Frye, S.V. (2010). The art of the chemical probe. Nat. Chem. Biol. *6*, 159–161.

Garrido, C., Brunet, M., Didelot, C., Zermati, Y., Schmitt, E., and Kroemer, G. (2006). Heat shock proteins 27 and 70: anti-apoptotic proteins with tumorigenic properties. Cell Cycle *5*, 2592–2601.

Gassler, C.S., Wiederkehr, T., Brehmer, D., Bukau, B., and Mayer, M.P. (2001). Bag-1M accelerates nucleotide release for human Hsc70 and Hsp70 and can act concentration-dependent as positive and negative cofactor. J. Biol. Chem. *276*, 32538–32544.

Goloudina, A.R., Demidov, O.N., and Garrido, C. (2012). Inhibition of HSP70: a challenging anti-cancer strategy. Cancer Lett. *325*, 117–124.

Hoepfner, D., Helliwell, S.B., Sadlish, H., Schuierer, S., Filipuzzi, I., Brachat, S., Bhullar, B., Plikat, U., Abraham, Y., Altorfer, M., et al. (2014). High-resolution chemical dissection of a model eukaryote reveals targets, pathways and gene functions. Microbiol. Res. *169*, 107–120.

Jiang, J., Prasad, K., Lafer, E.M., and Sousa, R. (2005). Structural basis of interdomain communication in the Hsc70 chaperone. Mol. Cell *20*, 513–524.

Kang, Y., Taldone, T., Patel, H.J., Patel, P.D., Rodina, A., Gozman, A., Maharaj, R., Clement, C.C., Patel, M.R., Brodsky, J.L., et al. (2014). Heat shock protein 70 inhibitors. 1. 2,5′-thiodipyrimidine and 5-(phenylthio)pyrimidine acrylamides as irreversible binders to an allosteric site on heat shock protein 70. J. Med. Chem. *57*, 1188–1207.

Karzai, A.W., and McMacken, R. (1996). A bipartite signaling mechanism involved in DnaJ-mediated activation of the Escherichia coli DnaK protein. J. Biol. Chem. *271*, 11236–11246.

Kityk, R., Kopp, J., Sinning, I., and Mayer, M.P. (2012). Structure and dynamics of the ATP-bound open conformation of Hsp70 chaperones. Mol. Cell *48*, 863–874.

Laufen, T., Mayer, M.P., Beisel, C., Klostermeier, D., Mogk, A., Reinstein, J., and Bukau, B. (1999). Mechanism of regulation of hsp70 chaperones by DnaJ cochaperones. Proc. Natl. Acad. Sci. USA *96*, 5452–5457.

Leu, J.I., Pimkina, J., Frank, A., Murphy, M.E., and George, D.L. (2009). A small molecule inhibitor of inducible heat shock protein 70. Mol. Cell *36*, 15–27.

Leu, J.I., Zhang, P., Murphy, M.E., Marmorstein, R., and George, D.L. (2014). Structural basis for the inhibition of HSP70 and DnaK chaperones by small-molecule targeting of a C-terminal allosteric pocket. ACS Chem. Biol. *9*, 2508–2516.

Liu, Q., and Hendrickson, W.A. (2007). Insights into Hsp70 chaperone activity from a crystal structure of the yeast Hsp110 Sse1. Cell *131*, 106–120.

Mayer, M.P., and Bukau, B. (2005). Hsp70 chaperones: cellular functions and molecular mechanism. Cell. Mol. Life Sci. *62*, 670–684.

Mayer, M.P., Laufen, T., Paal, K., McCarty, J.S., and Bukau, B. (1999). Investigation of the interaction between DnaK and DnaJ by surface plasmon resonance spectroscopy. J. Mol. Biol. *289*, 1131–1144.

Menezes, D.L., Taverna, P., Jensen, M.R., Abrams, T., Stuart, D., Yu, G.K., Duhl, D., Machajewski, T., Sellers, W.R., Pryer, N.K., and Gao, Z. (2012). The novel oral Hsp90 inhibitor NVP-HSP990 exhibits potent and broad-spectrum antitumor activities in vitro and in vivo. Mol. Cancer Ther. *11*, 730–739.

Montgomery, D.L., Morimoto, R.I., and Gierasch, L.M. (1999). Mutations in the substrate binding domain of the Escherichia coli 70 kDa molecular chaperone, DnaK, which alter substrate affinity or interdomain coupling. J. Mol. Biol. *286*, 915–932.

Morshauser, R.C., Hu, W., Wang, H., Pang, Y., Flynn, G.C., and Zuiderweg, E.R. (1999). High-resolution solution structure of the 18 kDa substrate-binding domain of the mammalian chaperone protein Hsc70. J. Mol. Biol. *289*, 1387–1403.

Nadler, S.G., Tepper, M.A., Schacter, B., and Mazzucco, C.E. (1992). Interaction of the immunosuppressant deoxyspergualin with a member of the Hsp70 family of heat shock proteins. Science *258*, 484–486.

Otaka, M., Yamamoto, S., Ogasawara, K., Takaoka, Y., Noguchi, S., Miyazaki, T., Nakai, A., Odashima, M., Matsuhashi, T., Watanabe, S., and Itoh, H. (2007). The induction mechanism of the molecular chaperone HSP70 in the gastric mucosa by Geranylgeranylacetone (HSP-inducer). Biochem. Biophys. Res. Commun. *353*, 399–404.

Pierce, S.E., Davis, R.W., Nislow, C., and Giaever, G. (2007). Genome-wide analysis of barcoded Saccharomyces cerevisiae gene-deletion mutants in pooled cultures. Nat. Protoc. *2*, 2958–2974.

Powers, M.V., Clarke, P.A., and Workman, P. (2008). Dual targeting of HSC70 and HSP72 inhibits HSP90 function and induces tumor-specific apoptosis. Cancer Cell *14*, 250–262.

Raviol, H., Sadlish, H., Rodriguez, F., Mayer, M.P., and Bukau, B. (2006). Chaperone network in the yeast cytosol: Hsp110 is revealed as an Hsp70 nucleotide exchange factor. EMBO J. *25*, 2510–2518.

Rodina, A., Patel, P.D., Kang, Y., Patel, Y., Baaklini, I., Wong, M.J., Taldone, T., Yan, P., Yang, C., Maharaj, R., et al. (2013). Identification of an allosteric pocket on human hsp70 reveals a mode of inhibition of this therapeutically important protein. Chem. Biol. *20*, 1469–1480.

Rousaki, A., Miyata, Y., Jinwal, U.K., Dickey, C.A., Gestwicki, J.E., and Zuiderweg, E.R. (2011). Allosteric drugs: the interaction of antitumor compound MKT-077 with human Hsp70 chaperones. J. Mol. Biol. *411*, 614–632.

Schlecht, R., Scholz, S.R., Dahmen, H., Wegener, A., Sirrenberg, C., Musil, D., Bomke, J., Eggenweiler, H.M., Mayer, M.P., and Bukau, B. (2013). Functional analysis of Hsp70 inhibitors. PLoS ONE *8*, e78443.

Smith, A.M., Ammar, R., Nislow, C., and Giaever, G. (2010). A survey of yeast genomic assays for drug and target discovery. Pharmacol. Ther. *127*, 156–164.

Smock, R.G., Rivoire, O., Russ, W.P., Swain, J.F., Leibler, S., Ranganathan, R., and Gierasch, L.M. (2010). An interdomain sector mediating allostery in Hsp70 molecular chaperones. Mol. Syst. Biol. *6*, 414.

Taldone, T., Kang, Y., Patel, H.J., Patel, M.R., Patel, P.D., Rodina, A., Patel, Y., Gozman, A., Maharaj, R., Clement, C.C., et al. (2014). Heat shock protein 70 inhibitors. 2. 2,5′-thiodipyrimidines, 5-(phenylthio)pyrimidines, 2-(pyridin-3-ylthio)pyrimidines, and 3-(phenylthio)pyridines as reversible binders to an allosteric site on heat shock protein 70. J. Med. Chem. *57*, 1208–1224.

Theyssen, H., Schuster, H.P., Packschies, L., Bukau, B., and Reinstein, J. (1996). The second step of ATP binding to DnaK induces peptide release. J. Mol. Biol. *263*, 657–670.

Vogel, M., Bukau, B., and Mayer, M.P. (2006a). Allosteric regulation of Hsp70 chaperones by a proline switch. Mol. Cell *21*, 359–367.

Vogel, M., Mayer, M.P., and Bukau, B. (2006b). Allosteric regulation of Hsp70 chaperones involves a conserved interdomain linker. J. Biol. Chem. *281*, 38705–38711.

Wang, H., Kurochkin, A.V., Pang, Y., Hu, W., Flynn, G.C., and Zuiderweg, E.R. (1998). NMR solution structure of the 21 kDa chaperone protein DnaK substrate binding domain: a preview of chaperone-protein interaction. Biochemistry *37*, 7929–7940.

Wang, A.M., Miyata, Y., Klinedinst, S., Peng, H.M., Chua, J.P., Komiyama, T., Li, X., Morishima, Y., Merry, D.E., Pratt, W.B., et al. (2013). Activation of Hsp70 reduces neurotoxicity by promoting polyglutamine protein degradation. Nat. Chem. Biol. *9*, 112–118.

Whitesell, L., Mimnaugh, E.G., De Costa, B., Myers, C.E., and Neckers, L.M. (1994). Inhibition of heat shock protein HSP90-pp60v-src heteroprotein complex formation by benzoquinone ansamycins: essential role for stress proteins in oncogenic transformation. Proc. Natl. Acad. Sci. USA *91*, 8324–8328.

Williamson, D.S., Borgognoni, J., Clay, A., Daniels, Z., Dokurno, P., Drysdale, M.J., Foloppe, N., Francis, G.L., Graham, C.J., Howes, R., et al. (2009). Novel adenosine-derived inhibitors of 70 kDa heat shock protein, discovered through structure-based design. J. Med. Chem. *52*, 1510–1513.

Wisén, S., and Gestwicki, J.E. (2008). Identification of small molecules that modify the protein folding activity of heat shock protein 70. Anal. Biochem. *374*, 371–377.

Wisén, S., Bertelsen, E.B., Thompson, A.D., Patury, S., Ung, P., Chang, L., Evans, C.G., Walter, G.M., Wipf, P., Carlson, H.A., et al. (2010). Binding of a small molecule at a protein-protein interface regulates the chaperone activity of hsp70-hsp40. ACS Chem. Biol. *5*, 611–622.

Yamamoto, S., Nakano, S., Owari, K., Fuziwara, K., Ogawa, N., Otaka, M., Tamaki, K., Watanabe, S., Komatsuda, A., Wakui, H., et al. (2010). Gentamicin inhibits HSP70-assisted protein folding by interfering with substrate recognition. FEBS Lett. *584*, 645–651.

Zhu, X., Zhao, X., Burkholder, W.F., Gragerov, A., Ogata, C.M., Gottesman, M.E., and Hendrickson, W.A. (1996). Structural analysis of substrate binding by the molecular chaperone DnaK. Science *272*, 1606–1614.

Zhuravleva, A., Clerico, E.M., and Gierasch, L.M. (2012). An interdomain energetic tug-of-war creates the allosterically active state in Hsp70 molecular chaperones. Cell *151*, 1296–1307.

Zuiderweg, E.R., Bertelsen, E.B., Rousaki, A., Mayer, M.P., Gestwicki, J.E., and Ahmad, A. (2013). Allostery in the Hsp70 chaperone proteins. Top. Curr. Chem. *328*, 99–153.